Novel Excimer Formation of Pyrene in Micelles of a Crown Ether Surfactant

Nicholas J. Turro* and Ping-Lin Kuo

Department of Chemistry, Columbia University, New York, New York 10027 (Received: December 8, 1986)

At low pyrene concentration (1.2×10^{-5} M), a strong excimer emission is observed in aqueous solutions containing micelles of the crown ether surfactant decyl 18-crown-6 ($C_{10}O18C$). ^1H NMR spectra of aqueous micellar solutions of $C_{10}O18C$ and of a conventional nonionic surfactant (C_9PhE_{10}) containing solubilized pyrene, the measurements of time-resolved emission of pyrene in $C_{10}O18C$ and in C_9PhE_{10}, and the dependence of excimer formation on $C_{10}O18C$ concentration all suggest that pyrene in $C_{10}O18C$ micelles is localized near the crown ether ring. The inferred location of pyrene in $C_{10}O18C$ micelles is used to interpret the strong tendency to form excimers of pyrene in $C_{10}O18C$ micelles. Temperature and pressure effects on excimer emission with and without salt are interpreted in terms of changes in micelle structure.

Introduction

Crown ethers have attracted wide attention due to their outstanding ability to complex with cations and anions.[1] The attachment of a lipophilic long-chain alkyl group to a crown ether converts it to a crown ether surfactant which can form micelles similar to those of a conventional nonionic surfactant in aqueous solution.[2] The properties of such crown ether surfactants in aqueous solution have been studied in the presence and absence of salts,[3] and it has been found that the micellar properties and solution properties are significantly influenced by cation complexation.

Not only can crown ethers complex with cations and with anions but they can also associate with uncharged molecules via dipole–dipole interactions. For example, pyrene, a polarizable compound, is able to bind 18-crown-6 units that are anchored onto a polymer backbone.[4] In our study, a very strong pyrene excimer emission has been found from pyrene solubilized in aqueous solutions of a crown ether surfactant. These results are attributed to the interaction between the crown ether group and pyrene based on the results from NMR and time-resolved emission measurements. It was found that variations of temperature, pressure, and the concentration of crown ether surfactant influence the properties of the crown ether surfactant, which in turn, influence the interaction between the crown ether and pyrene. The relations among these effects are correlated with each other and compared to those for a conventional nonionic surfactant.

Experimental Section

Materials. Decyl 18-crown-6 ($C_{10}O18C$) was a generous gift from Professor Okahara, Osaka University.[5] The syntheses of α,α'-1,3-dinaphthylpropane (DNP) is described in the literature.[6] Pyrene (P, Aldrich Chemical Co.) was purified by recrystallization from ethanol (three times). The selected poly(ethylene glycol) *n*-nonylphenyl ether (C_9PhE_{10}, Tokyo Kasei Co.), sodium dodecyl sulfate (SDS, electrophoresis grade, Bio-Rad Laboratories), and potassium chloride (Ultrapure grade, Alfa) were used as supplied.

Measurements of Pyrene Fluorescence. All of the fluorescence spectra were recorded on a SLM Instruments Model 8000 spectrophotometer. The optical densities (OD) of pyrene solutions were measured on a Perkin-Elmer 559A UV/visible spectrophotometer, and the time-resolved emission studies were performed employing a time-resolved laser spectrometer previously described.[7] The decay curve and lifetimes of micellized pyrene were acquired by the single photon counting technique.[8] The I_1/I_3 values of pyrene were used to measure the cmc of $C_{10}O18C$ in the presence of pyrene as described previously.[9] The ratio of the intensity of the maximum pyrene excimer emission (ca. 470 nm) to the maximum of pyrene monomer emission (375 nm) is defined as I_e/I_m. The internal excimer formation of DNP (I_e/I_m, the intensity ratio of monomer emission at 379 nm to excimer emission at 337 nm) was used to estimate the microviscosity of $C_{10}O18C$ and C_9PhE_{10} according to a reported method.[10] A previously described stainless steel high-pressure cell was used for high-pressure measurements.[11,12]

NMR Measurements. ^1H NMR spectra were measured on a Bruker WM-250 NMR spectrometer. The samples of $C_{10}O18C$ with and without pyrene possessed the same $C_{10}O18C$ concentrations and were measured under the same conditions. The peak of HOD at $\delta = 4.59$ was used as an internal standard assuming the temperatures of measurement for both samples were the same. The molar ratio of $C_{10}O18C$ to pyrene for the sample of $C_{10}O18C$ with pyrene was 10:1.

Results

The excimer emission of pyrene in aqueous solutions of SDS can be observed only at fairly high pyrene concentrations; e.g., I_e/I_m is ca. 0.4 at a pyrene concentration of 3×10^{-4} M, whereas at a pyrene concentration of 1.2×10^{-5} M, in SDS (50 mM), virtually no excimer emission can be observed. However, at this same low pyrene concentration, pyrene shows a strong excimer emission in $C_{10}O18C$ (2 mM) with an I_e/I_m value of 0.47; but in aqueous solution of the conventional nonionic surfactant C_9PhE_{10}, pyrene does not show any excimer emission at concentration of ca. 10^{-5} M (Figure 1).

The I_e/I_m value changes as a function of $C_{10}O18C$ concentration (Figure 2) and passes through a maximum. For these experiments, the pyrene concentration and OD (ca. 0.1) of the system were kept constant. Even at as low a pyrene concentration as 2.2×10^{-6} M, excimer emission can be observed below the cmc of $C_{10}O18C$. At this pyrene concentration, the cmc can be read to be ca. 3×10^{-4} M from the inflection point of the plot of I_1/I_3 vs. log $[C_{10}O18C]$ (Figure 2). The maximum value of I_e/I_m is observed close to cmc.

(1) Christensen, J. J. In *Bioenergetics and Thermodynamics, Model Systems*; Braibanti, A., Ed.; Reidel: Dordrecht, The Netherlands, 1980.

(2) (a) LeMoigne, J.; Gramian, Ph.; Simon, J. *J. J. Colloid Interface Sci.* **1977,** *60,* 565. (b) Morio, Y.; Pramauro, E.; Gratzel, M.; Pelizzetti, E.; Tundo, P. *J. Colloid Interface Sci.* **1979,** *69,* 341. (c) Winter, H.-J.; Manecke, G. *Makromol. Chem.* **1985,** *186,* 1979.

(3) (a) Kuo, P.-L.; Ikeda, I.; Okahara, M. *Tenside Deterg.* **1982,** *19,* 4. (b) Kuo, P.-L.; Ikeda, I.; Okahara, M. *Tenside Deterg.* **1982,** *19,* 204. (c) Kuo, P.-L.; Tsuchiya, K.; Ikeda, I.; Okahara, M. *J. Colloid Interface Sci.* **1983,** *92,* 463.

(4) Roland, B.; Kimura, K.; Smid, J. *J. Colloid Interface Sci.* **1984,** *97,* 392.

(5) Ikeda, I.; Yamamura, S.; Nakatsuji, Y.; Okahara, M. *J. Org. Chem.* **1980,** *45,* 5355.

(6) Chandross, E. A.; Dempster, C. J. *J. Am. Chem. Soc.* **1970,** *92,* 3586.

(7) Turro, N. J.; Aikawa, M.; Butcher, J. A. *IEEE J. Quantum Electronics* **1980,** *QE-16,* 1218.

(8) Turro, N. J.; Aikawa, M. *J. Am. Chem. Soc.* **1980,** *102,* 4866.

(9) Turro, N.J.; Kuo, P.-L. *J. Phys. Chem.* **1986,** *90,* 837.

(10) Avouris, P.; Kordas, J.; El-Bayoumi, M. A. *Chem. Phys. Lett.* **1974,** *26,* 373.

(11) Turro, N. J.; Okubo, T. *J. Am. Chem. Soc.* **1981,** *103,* 7224.

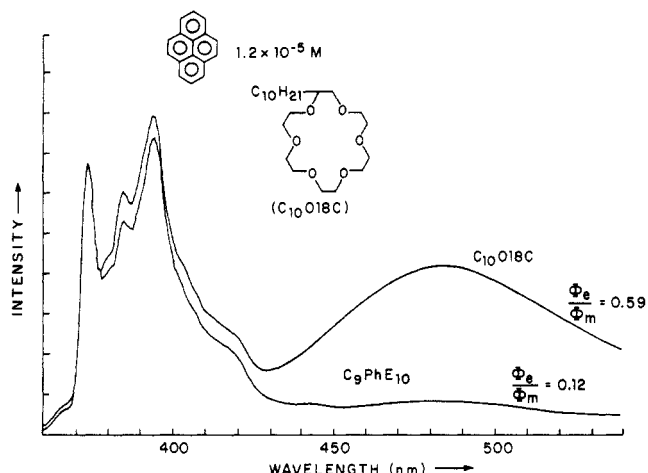(12) Gratzel, M.; Kalyanasundaram, K.; Thomas, J. K. *J. Am. Chem. Soc.* **1974,** *96,* 7869.

Figure 1. Emission spectra of pyrene (1.2×10^{-5} M) in aqueous solutions of $C_{10}O18C$ (2 mM) and C_9PhE_{10} (2 mM).
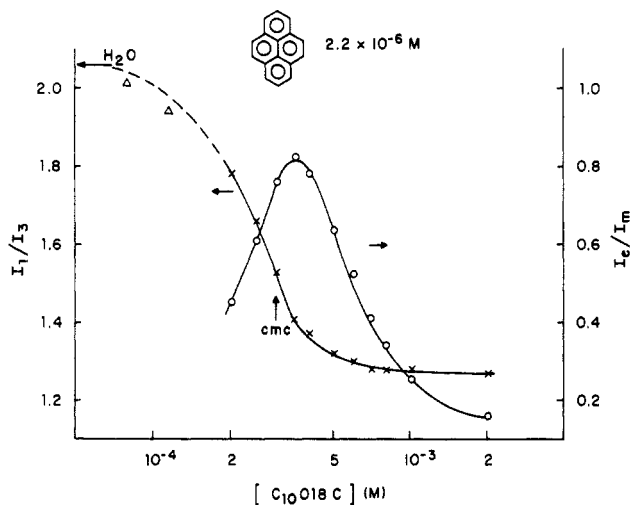
Figure 2. Variations of I_e/I_m and I_1/I_3 of pyrene in $C_{10}O18C$ as a function of $C_{10}O18C$ concentration. The Δ points are taken from data in ref 9.
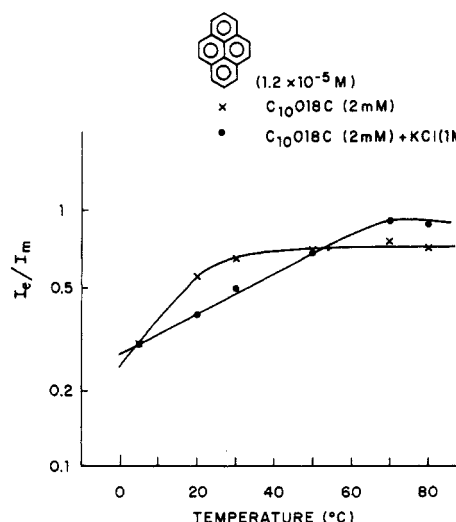

Figure 3. Temperature effect on the excimer emission (I_e/I_m) of pyrene in $C_{10}O18C$ with and without KCl.

Figure 3 shows the temperature effect on the I_e/I_m of pyrene in $C_{10}O18C$ in the presence and absence of KCl. Without KCl, the λ_{max} of excimer emission shifts from ca. 475 nm at 5 °C to 469 nm at 70 °C. The I_e/I_m value increases with increasing temperature and then reaches a plateau at 25 °C. In the presence of KCl, the extent of excimer emission varies in a similar manner as a function of temperature. The increasing value of I_e/I_m upon
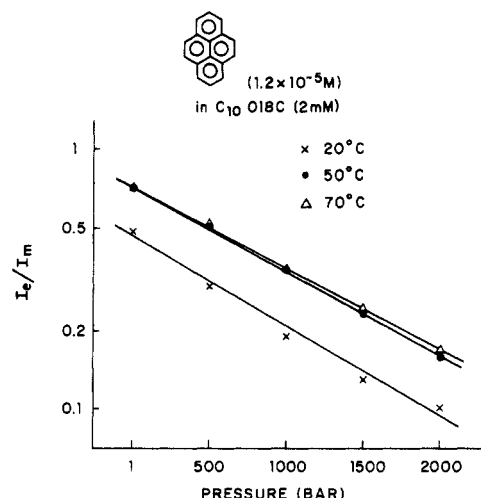

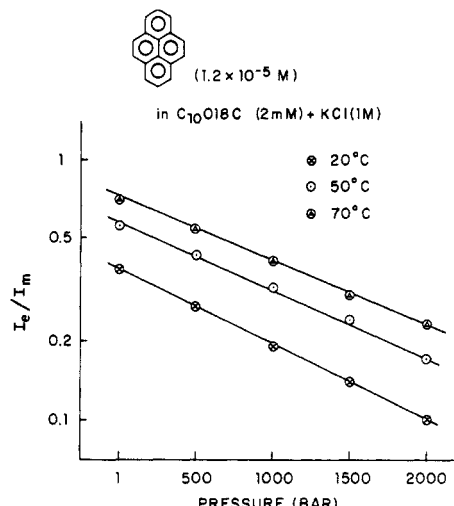**Figure 4.** Pressure effect on the excimer emission (I_e/I_m) of pyrene in $C_{10}O18C$.

Figure 5. Pressure effect on the excimer emission (I_e/I_m) of pyrene in $C_{10}O18C$ with added KCl.

increasing temperature is also followed by a plateau at ca. 70 °C. The break points on the two plots are found to correspond to the cloud points of aqueous solutions of $C_{10}O18C$ without and with KCl, respectively. At 20 °C, the aqueous solution of $C_{10}O18C$ with and without KCl is transparent. The addition of KCl decreases the I_e/I_m value.

Figures 4 and 5 show the pressure effect on the I_e/I_m of pyrene in $C_{10}O18C$ without and with KCl at 20, 50, and 70 °C, respectively. For each case, the I_e/I_m value decreases with increasing pressure, and a linear relation between log I_e/I_m and pressure is observed. The I_e/I_m value at 50 °C and that at 70 °C under various pressures overlap with each other in the absence of KCl but do not overlap in the presence of KCl. This result is consistent with the temperature effect on I_e/I_m under atmospheric pressure (Figure 3). With and without KCl, I_e/I_m is slightly more sensitive to pressure at low temperature; i.e., the slope of the plot of log I_e/I_m vs. P is higher at low temperature.

The ^{1}H NMR method[13] was used to qualitatively study the time-average location of pyrene inside the micelles of $C_{10}O18C$ and C_9PhE_{10}. For C_9PhE_{10}, the protons both poly(oxyethylene) and the hydrophobic group are influenced by pyrene, suggesting that, on a time average, pyrene is distributed throughout the whole of the micelle. For $C_{10}O18C$, however, the proton absorption of oxyethylene is split into two pairs (Figure 6) and is significantly shifted by pyrene. This result suggests that, on a time average, pyrene is located near the crown ether ring of $C_{10}O18C$ relative

(13) Schick, M. J.; Atlas, S. M.; Eirich, F. R. *J. Phys. Chem.* **1962**, *66*, 1326.

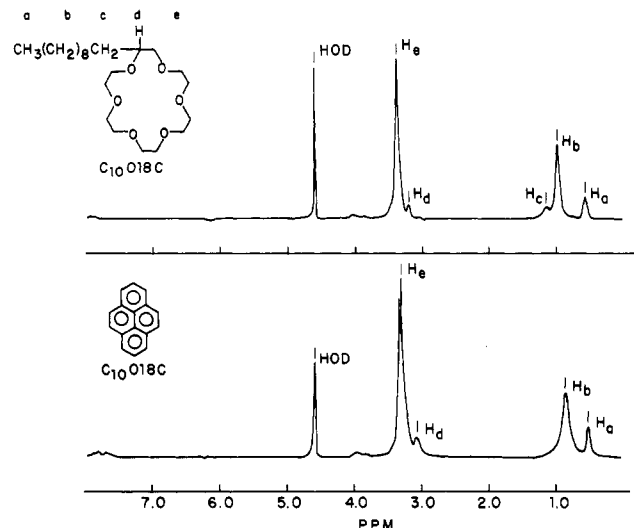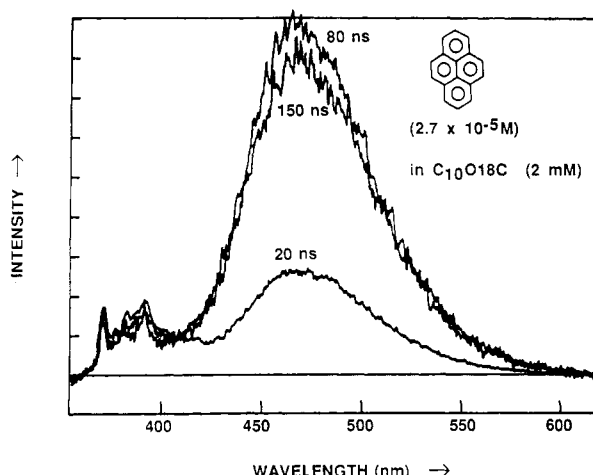**Figure 6.** ^{1}H NMR spectra of $C_{10}O18C$ in the presence and absence of pyrene.

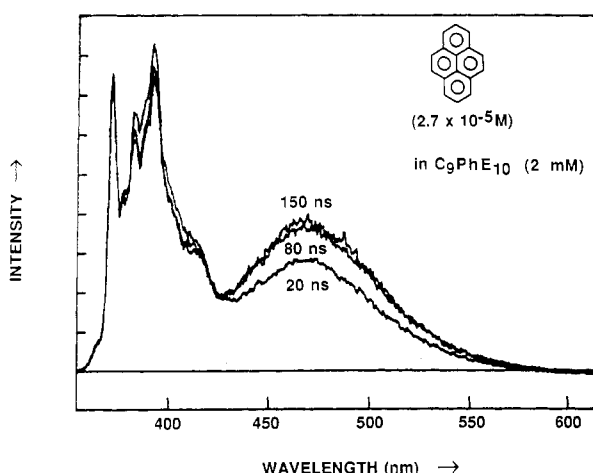**Figure 7.** Time-resolved emission spectra of pyrene (normalized at 375 nm) in $C_{10}O18C$ at 20, 80, and 150 ns.

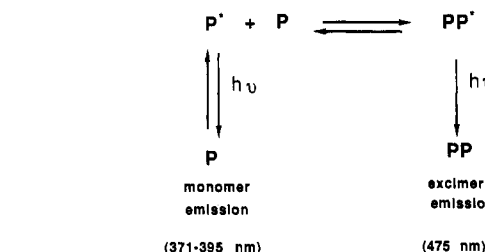**Figure 8.** Time-resolved mission spectra of pyrene (normalized at 375 nm) in C_9PhE_{10} at 20, 80, and 150 ns.

to the poly(oxyethylene) group of C_9PhE_{10}.

Time-resolved emission was employed to investigate the dynamic properties of the pyrene probe at very short time intervals. Figures 7 and 8 show the time-resolved emission spectra of pyrene excimer in $C_{10}O18C$ and in C_9PhE_{10} at 20, 80, and 150 ns after pulsed laser excitation. The OD of each sample was adjusted to 1.2 so that the excimer emission could be observed for C_9PhE_{10}. At OD = 1.2, the occupancy number of pyrene in $C_{10}O18C$ (1.2) is much

TABLE I: Time-Resolved Emission of Pyrene (I_e/I_m) in $C_{10}O18C$ and C_9PhE_{10}

	t, ms					
	20	60	80	100	150	∞
C10O18C	1.53	3.60	5.00	4.70	4.30	2.50
C9PhE10	0.39	0.46	0.49	0.53	0.54	0.58

SCHEME I: Mechanism for Monomer and Excimer Emission^a

^{a}According to this mechanism the excitation spectra for excimer emission is the same as that for monomer emission
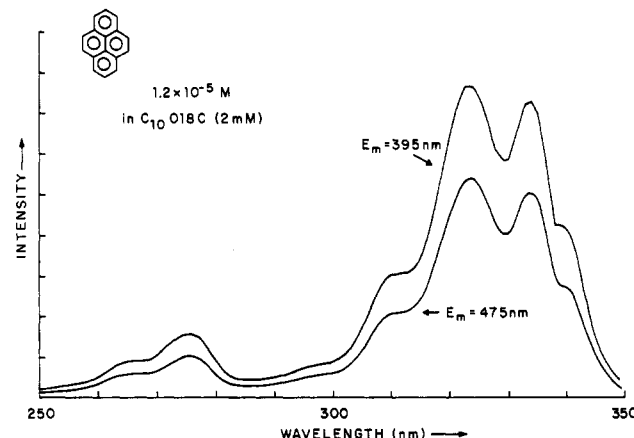

Figure 9. Excitation spectra of pyrene for excimer emission (475 nm) and for monomer emission (395 nm).

smaller than that in C_9PhE_{10} (3.8). At each time interval, the I_e/I_m value in $C_{10}O18C$ is higher than that in C_9PhE_{10} (Table I). In C_9PhE_{10}, the I_e/I_m increases with increasing time and reaches a maximum ($I_e/I_m = 0.54$) at ca. 150 ns. This maximum value is close to the I_e/I_m value for the steady-state emission ($I_e/I_m = 0.58$) suggesting that excimer formation reaches equilibrium on a time scale longer than 150 ns. In $C_{10}O18C$, the I_e/I_m value passes through a maximum at 80 ns, and the I_e/I_m value at 150 ns (4.3) is still much higher than that of steady state ($I_e/I_m = 2.5$).

Discussion

According to Scheme I, if the emission at 475 nm is from the pyrene excimer (PP*) derived from P*, the excitation spectra for the emission maximum at 475 nm must be the same as that for P* whose emission maximum is at 395 nm. On the other hand, if the excimer emission at 475 nm is from excited pyrene aggregates or crystallites (P_n*), its excitation spectrum is expected to be different from that for P*. In a separate experiment with an aqueous solution of $C_{10}O18C$ containing pyrene precipitates (P_n), an emission at ca. 475 nm can be observed. However, the excitation spectrum for the emission at 475 nm is different from that for monomer emission. For the pyrene excimer in $C_{10}O18C$ in Figure 1, the excitation spectra for excimer emission (475 nm) and for monomer emission (395 nm) show the same shape and wavelength of absorption (Figure 9), suggesting that the emission at ca. 475 nm observed for pyrene in $C_{10}O18C$ is from the excimer emission (PP*) and not from undissolved pyrene aggregates or crystallites.

The three significant conventional factors influencing the possibility for pyrene to form excimers in micelles are (1) the

occupancy number (n) of pyrene molecules in a micelle; (2) the microviscosity experienced by a pyrene molecule inside the micelle (η); and (3) the lifetime (τ_{av}) of pyrene in a micelle. Our results are discussed in terms of these factors for $C_{10}O18C$ and for C_9PhE_{10}.

A higher n value will increase the probability for an excited pyrene (P*) to collide with a ground-state pyrene (P) during its lifetime τ_{av} to form an excimer. In Figure 1, the calculated occupancy numbers for pyrene in $C_{10}O18C$ and in C_9PhE_{10} are 0.52 and 1.72, based on their aggregation numbers[9,13] of 88 and 276, respectively. Thus, we conclude that the larger value of I_e/I_m for $C_{10}O18C$ does not result from a larger value of n in the crown ether surfactant micelles.

In a specific environment, a longer lifetime of P* will increase the probability for P* to collide with P to form an excimer. The lifetime of pyrene in $C_{10}O18C$ (162 ns), however, is shorter than that in C_9PhE_{10} (204 ns). Thus the larger value of I_e/I_m for $C_{10}O18C$ does not result from a larger lifetime of pyrene in the crown ether surfactant micelles.

A higher microviscosity of the micelle reduces the diffusion rate of pyrene inside the micelles and decreases the probability of forming excimers. The intramolecular formation of excimers by DNP has been used to estimate the microviscosity inside a micelle.[9] The higher the I_e'/I_m' value DNP displays, the lower the viscosity it experiences inside a micelle. The I_e'/I_m' value of DNP in $C_{10}O18C$ and in C_9PhE_{10} corresponds to microviscosities of 71 and 48 cP, respectively, according to a calibration curve in which the values of I_e'/I_m' were determined for homogeneous solvents of known viscosity.[10] Thus, the larger value of I_e/I_m in $C_{10}O18C$ compared to C_9PhE_{10} does not result from a lower microviscosity of the crown ether surfactant micelles.

The conventional factors of occupancy number, microviscosity, and lifetime do not favor pyrene excimer formation in $C_{10}O18C$. Thus, we conclude that the strong excimer emission for pyrene in $C_{10}O18C$ is due to a novel factor or factors.

The hydrophilic group of $C_{10}O18C$ is the 18-crown-6 crown ring consisting of six symmetrically separated oxygen atoms with a diameter of ca. 7.8 Å.[14] Pyrene is a flat molecule composed of four aromatic rings with a diameter of ca. 7.9 Å which is similar to the size of the crown ring. The similarity of the sizes between 18-crown-6 and pyrene and the polarizability of pyrene are factors that could cause an effective interaction. The ^1H NMR spectra show that, on a time average, pyrene is located near the crown ether ring inside the micelle of $C_{10}O18C$. These results provide support for the existence of a specific interaction between the crown ether ring and pyrene. The reported binding[4] of pyrene to polymer-anchored 18-crown-6 also suggests the existence of such an interaction. This "sandwich" type of interaction between the 18-crown-6 unit of $C_{10}O18C$ and pyrene increases the probability for pyrene to be located in the vicinity of the hydrophilic head group instead of being delocalized over the whole micelle. Thus, the effective local concentration of pyrene in $C_{10}O18C$ micelle near the head groups is higher than that in a C_9PhE_{10} micelle with the same occupancy number because of the delocalized nature of pyrene in the latter micelle. The higher local concentration explains the strong excimer formation observed in $C_{10}O18C$ micelles relative to that observed in C_9PhE_{10} micelles.

Even at short time intervals after excitation (20, 60, 80, 100, and 150 ns), the measurement of time-resolved emission (Figures 7 and 8) shows stronger excimer emission in $C_{10}O18C$ than in C_9PhE_{10}. This result can also be ascribed to the higher local concentration of pyrene inside $C_{10}O18C$ micelles in spite of the lower occupancy number. In C_9PhE_{10}, however, the value of I_e/I_m increases in the same increasing time intervals and reaches a stable value close to that of steady state. The probability for P* to collide with P to form an excimer is greater in the longer time intervals. In $C_{10}O18C$, I_e/I_m value reaches a maximum during a relatively short time interval (80 ns) due to the high local concentration. After 80 ns, the value of I_e/I_m continually decreases. This observation may be due to the depletion of multiply occupied micelles

(14) Frensdorff, H. K. *J. Am. Chem. Soc.* **1971**, *93*, 600.

SCHEME II: Mechanism for Pyrene Excimer Formation at Different $C_{10}O18C$ Concentrations

Below cmc   At cmc   Above cmc
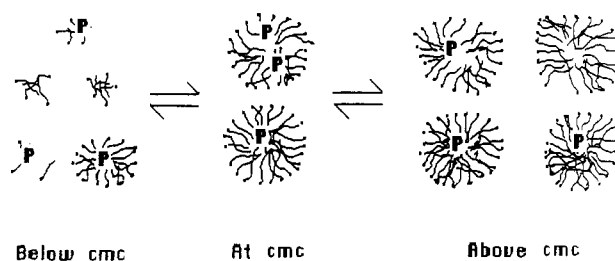
and the onset of a new rate-determining step such as pyrene exchange between micelles. Further experimentation is needed to elaborate this issue.

The existence of a significant interaction between the crown ether ring and pyrene also can be used to interpret the maximum observed in the plot of I_e/I_m vs. log $[C_{10}O18C]$ (Figure 2). Scheme II is used to interpret the mechanism of pyrene excimer formation at different $C_{10}O18C$ concentrations. Below the cmc, we postulate that $C_{10}O18C$ forms premicelles which are not full-sized micelles but consist of only several $C_{10}O18C$ molecules; these premicelles are in equilibrium with larger or "full-sized" micelles. The specific interaction between pyrene and the crown ether causes larger numbers of these premicelles to form. As a result, the value I_e/I_m is small because the concentration of pyrene is small locally. As the concentration of crown ether surfactant is increased, "full-sized" micelles increase in number and pyrene molecules are transferred from the separated premicelles to full-sized micelles. As the cmc is approached the number of micelles with two (or more) pyrene molecules begins to increase and the I_e/I_m value also increases. Above the cmc the number of "full-sized" micelles begins to increase and the number of micelles containing two or more pyrene molecules begins to decrease and the value of I_e/I_m decreases. Thus, above the cmc, the I_e/I_m decreases with increasing $[C_{10}O18C]$ simply because of the decreasing occupancy number; i.e., at a fixed concentration of pyrene, an increase in the number of micelles decreases the fraction of micelles containing two pyrene molecules.

An increase in temperature increases the occupancy number as a result of the increase in micelle size, which reduces the number of micelles, and also increases the diffusion rate of pyrene inside the micelles.[15] Therefore, increasing the temperature favors excimer formation and increases the I_e/I_m value. The increasing I_e/I_m value above the cloud point is also probably due to the increasing micellar size. For solution at 20 °C, the addition of KCl decreases I_e/I_m. This is probably due to the decrease in occupancy number as a result of a decrease in micellar size in the presence of salt.

The pressure effect on I_e/I_m of pyrene in $C_{10}O18C$ is qualitatively the same as that in C_9PhE_{10}. Increasing pressure decreases the occupancy number as a result of a decrease in micellar size upon increasing pressure[16] and thus causes a decrease in I_e/I_m.

Conclusion

At low pyrene concentration (1.2×10^{-5} M), a strong excimer emission in $C_{10}O18C$ is observed. The excitation spectra for both the monomer emission (395 nm) and the excimer emission (475 nm) are the same, suggesting that the emission maximum at 475 nm is not due to pyrene aggregates. The I_e/I_m values change as a function of $C_{10}O18C$ concentration and pass through a maximum. For ^1H NMR spectra in $C_{10}O18C$, the protons of the crown ether unit are shifted most significantly, whereas in C_9PhE_{10}, protons at all sites are shifted but to a lesser degree. The results of time-resolved emission of pyrene in $C_{10}O18C$ and in C_9PhE_{10} show that it is easier for pyrene to form excimers in $C_{10}O18C$ at

(15) (a) Nakagawa, T. *Nonionic Surfactants*; Schick, M. J., Eds.; Dekker: New York, 1967; p 558. (b) Mankowick, A. M. *J. Am. Oil Chem. Soc.* **1965**, *42*, 185.

(16) Nishikido, N.; Shinozaki, Y.; Sugihara, G.; Tanaka, M. *J. Colloid Interface Sci.* **1980**, *74*, 474.

short time intervals. These results are interpreted to mean that pyrene in $C_{10}O18C$ is localized near the crown ether ring due to the interaction between pyrene and the crown ether ring of the surfactant. The localization increases the effective pyrene concentration needed for excimer formation and therefore increases the probability of pyrene excimer formation. Temperture and pressure effects on I_e/I_m of pyrene in $C_{10}O18C$ with and without KCI are consistent with expected changes in micellar aggregation numbers under different temperature and pressure conditions.

Effects of Structural and Chemical Characteristics of Zeolites on the Properties of Their Bridging Hydroxyl Groups

A. G. Pelmenshchikov, V. I. Pavlov, G. M. Zhidomirov,

Institute of Catalysis, USSR Academy of Sciences, 630090 Novosibirsk 90, USSR

and S. Beran*

The J. Heyrovský Institute of Physical Chemistry and Electrochemistry, Czechoslovak Academy of Sciences, Máchova 7, 121 38 Prague 2, Czechoslovakia (Received: December 8, 1986)

The nonempirical SCF method with a STO-3G basis set is used to study the effects of the geometry (SiO and AlO bond lengths and SiOAl angles) and chemical (the Si:Al ratio) characteristics of zeolites on the vibrational frequencies of their OH groups modeled by the $H_3SiOHAlH_3$, $H_3SiOSi(OH)_3$, and $H_2AlOSi(OH)_3$ molecules. It is shown that the values of the vibrational frequencies are particularly affected by the structural characteristics (e.g., changes in the Si–O and Al–O bond lengths and the SiOAl angle of 0.04×10^{-10} m and 20°, respectively, result in shifts of the stretching frequency ν_{OH} of up to 40 cm^{-1}), while the influence of the chemical composition of zeolites is negligibly small (e.g., a substitution of Al for Si in the third coordination sphere of OH leads to a change of about 1 cm^{-1}).

Introduction

This paper deals with the influence of the geometrical characteristics of chemically identical fragments, particularly bridging OH groups, >SiOHAl<, in zeolites, on the vibrational frequencies ν_{OH}. This factor has not so far been taken into account in the interpretation of IR data for various zeolites. Moreover, some authors,[1,2] refering to the results of CNDO/2 calculations,[3] concluded that the effect of the structural characteristics of the >SiOHAl< fragment on the stretching vibrational frequencies ν_{OH} is negligibly small. Because of other factors which simultaneously affect the ν_{OH} frequency (see below) it is practically impossible to confirm or refute this conclusion on the basis of the experimental data available on zeolites. On the other hand, there is a whole series of analogous examples in IR spectroscopy of molecules which seem to contradict the conclusion in ref 3. For example, variations in the CCC angle in the >CCH$_2$C< fragment in cyclobutane ($\angle$CCC = 60°), cyclopentane ($\angle$CCC = 90°), and cyclohexane ($\angle$CCC = 108°) lead to the following values of the asymmetric, $\nu_{CH_2}^{as}$, or symmetric, $\nu_{CH_2}^{sym}$, vibrational frequencies: $\nu_{CH_2}^{as}$ = 3081, 2981, and 2952 cm^{-1} or $\nu_{CH_2}^{sym}$ = 3013, 2870, and 2866 cm^{-1}, respectively.[4] The SiOAl angle in the similar >SiOHAl< fragment also varies by about 40°, depending on its position in the zeolite framework. The difference in the geometry of both the >CCH$_2$C< fragment in a series of molecules and the >SiOHAl< fragment in different sites of the zeolite framework originates from the steric deformations. Reviewing the influence of the geometrical factor on the vibrational frequencies of the chemically identical fragments in various organic molecules,

Bellamy showed[4] that the variation in the frequencies is connected with the changes in the hybridization of the atomic orbitals on the C atom. Theoretical discussion of the effect of the hybridization of the atomic orbitals on the O atom on the properties of its bonds is given in ref 5 and 6. For the reasons mentioned above, the role of the structural factors will be discussed in this article.

However, to complete the picture of this phenomenon, it should be noted that the presence of different frequencies of the OH groups observed for various oxides has so far been assumed to be connected with a chemical factor; i.e., with changes in the chemical composition of the fragments to which the OH group is bonded. In this case, it is important to known the manner in which the vibrational frequency, ν_{OH}, depends on the mutual arrangement of the OH group and the position in which a substitution of an atom takes place. Tsyganenko showed[7] that the value of the vibrational frequency of OH groups in M_mO_n oxides is associated with the number and type of M atoms bonded to this group; i.e., it depends only on the chemical properties of the atoms situated in the first coordination sphere of the OH group. As the coordination number of an OH group does not exceed 3, Knözinger explained the higher number of the vibrational frequencies of OH groups on alumina by taking into account the coordination numbers of the Al atoms bonded to the OH group; i.e., the second coordination sphere of the OH group was considered.[8] With zeolites, the variation of the vibrational frequencies of the bridging OH groups was accounted for by the different distribution of the T = Si or Al atoms in the (>TO)$_3$SiOHAl< fragments; i.e., by the different composition of the third coordination sphere.[9]

(1) Jacobs, P. A.; Mortier, W. J. *Zeolites* **1982,** *2,* 227.
(2) Mortier, W. J.; Sauer, J.; Lercher, J. A.; Noller, H. *J. Phys. Chem.* **1984,** *88,* 905.
(3) Mortier, W. J.; Geerlings, P. *J. Phys. Chem.* **1982,** *84,* 1980.
(4) Bellamy, L. J. *The Infra-Red Spectra of Complex Molecules,* 2nd ed; Methuen: London, 1958.

(5) Newton, M. D.; Gibbs, G. V. *J. Phys. Chem. Miner.* **1980,** *6,* 221.
(6) Newton, M. D. *Structure and Bonding in Crystals,* Vol. 1, O'Keefe, M., Navrotsky, A., Eds.; Academic: New York, 1981.
(7) Tsyganenko, A. A.; Felimov, V. N. *J. Mol. Struct.* **1973,** *19,* 579.
(8) Knözinger, H.; Ratnasamy, P. *Catal Rev. Sci. Eng.* **1978,** *17,* 31.
(9) Von Balmoos, R.; Meier, W. H. *Nature (London)* **1981,** *289,* 782.